Computational Molecular Modeling of Polymer Solid Electrolytes II: Multiscale Molecular Modeling of Amorphous Polyethylene oxide

Visit Vao-soongnern[1,2], Supagorn Rugmai[3,4], Wanata Klysubun[4]

Laboratory of Computational and Applied Polymer Science[1], School of Chemistry[2], School of Physics[3], Institute of Science, Suranaree University of Technology, National Synchroton Research Center[4], Nakhon Ratchasima, 30000

Abstract

The development of computational methods for predicting structures and properties of polymers from chemical constitution calls for hierarchical strategies, capable of addressing the broad spectra of length and time scales governing the behavior of these materials. To address these challenges, multi-scale modeling techniques have been developed. This work present a recently developed strategy that has used a method where an atomistic chain is mapped onto a coarse-grained model and then reverse-mapped back to a fully atomistic system. Polyethylene oxide (PEO) model which each bead represents series of linked vectors connecting the CH_2CH_2 and CH_2O units was constructed. Beads located at the midpoint of each vector define centers for long range interaction energies between monomer subunits. Next, a bulk simulation is performed with a dynamic Monte Carlo procedure to equilibrate the structure. Then, energy minimization was performed, thereby generating an off-lattice replica in continuous space. Static properties include thermodynamic properties, such as material cohesive energy densities, structural properties as embodied in the pair/radial distribution, conformational distribution and X-ray/Neutron scattering curves were reported. The calculated solubility parameters for poly(ethylene oxide) is 10.02 $cal^{1/2}/cm^{3/2}$ which is in good agreement with the literature values (9.8 $cal^{1/2}/cm^{3/2}$). Other simulated properties are also comparable to reported experimental values.

Introduction

Within the last 20 years, many research institutions have recognized the need for a more systematic approach to new materials development that employs a multiscale modeling approach. Computational Materials draws from physics and chemistry, but focuses on constitutive descriptions of materials that are useful in formulating macroscopic models of material performance. The benefits of this technique are two folds. First, it encourages a reduced reliance on costly trial and error to materials research. Second, it increases the confidence that new materials will possess the desired properties when scaled up from the laboratory level, so that lead-time for the introduction of new technologies is reduced. For the case of polymeric materials, the development of computational methods for predicting structures and properties from chemical constitution calls for hierarchical strategies, capable of addressing the broad spectra of length and time scales governing the behavior of these materials. To address these challenges, multi-scale modeling techniques have been developed. This path consists of three steps: (i) mapping of an atomistic system onto a coarse-grained representation on a sparsely occupied high coordination lattice (ii)

performing MC simulations on the high coordination lattice and (iii) reverse mapping of selected snapshots from the high coordination lattice back to an atomistic system. Then, energy minimization of these reverse-mapped snapshots can be rapidly performed, thereby generating an off-lattice replica in continuous space. In this work, we generate a large equilibrium structure of amorphous polyethylene oxide (PEO). This theoretical prediction will be employed as a fitting model for PEO/Salt electrolytes nanostructure based on Extended X-Ray Absorption Fine Structure (EXAFS) technique at National Synchroton Research Center (NSRC), Nakhon Ratchasima.

Simulation Method and Details

Model The Monte Carlo simulations were performed on a high coordination lattice using coarse-grained PEO chains. This lattice, which is constructed by eliminating every other site from a diamond lattice, has a coordination number of 12, which provides flexibility to define a rotational state on the lattice. PEO chain is represented by a coarse-grained CH_2CH_2 or CH_2O beads, connected by coarse-grained bonds of length 2.39 Å. On this lattice, the angle between any two axes along the sides of the unit cell is 60°, and the lattice sites are identical to the hexagonal packing of hard spheres.

Energies Both short-range intramolecular interactions and long-range intra- and intermolecular interactions were introduced into the current simulations. The short-range intramolecular interactions resulting from the local chain conformation are based on a Rotational Isomeric State (RIS) model for the unperturbed chain, which incorporates the influence of partial charges. The RIS model for poly(A-A-B) chains, in which all bonds are subject to a symmetric 3-fold torsion potential with the nearest neighbor interdependence, is given by the following three statistical weight matrices for three successive bonds of type A-A, A-B, and B-A.

$$U_{AA} = \begin{bmatrix} 1 & \sigma_{BB} & \sigma_{BB} \\ 1 & \sigma_{BB} & \sigma_{BB}\omega_{AB} \\ 1 & \sigma_{BB}\omega_{AB} & \sigma_{BB} \end{bmatrix} \qquad U_{AB} = \begin{bmatrix} 1 & \sigma_{AA} & \sigma_{AA} \\ 1 & \sigma_{AA} & \sigma_{AA}\omega_{AB} \\ 1 & \sigma_{AA}\omega_{AB} & \sigma_{AA} \end{bmatrix} \qquad U_{BA} = \begin{bmatrix} 1 & \sigma_{AA} & \sigma_{AA} \\ 1 & \sigma_{AA} & \sigma_{AA}\omega_{AA} \\ 1 & \sigma_{AA}\omega_{AA} & \sigma_{AA} \end{bmatrix}$$

In the matrices, the rows and columns define the states of bonds i - 1 and i, respectively. The three accessible rotational isomeric states for each bond are t, g^+, and g^-, used in this order in the matrices. The σ_{AA} and σ_{AB} are the statistical weights for the A-A and A-B type first-order interactions, and ω_{AA} and ω_{AB} represent the second-order interactions. They are calculated as Boltzmann factors using the energies calculated from an *ab initio* QM calculation in a preceding paper. The short-range interactions determine the local chain conformation for an unperturbed chain. The long-range interactions are obtained from a discretized form of the LJ potential, in which the second virial coefficient for polymers is evaluated similar to a nonideal gas using the Mayer f function. The LJ parameters (σ and ε) for two backbone atoms of PEO were estimated by fitting the experimental bulk density of PEO at a suitable temperature from a series of simulations of free-standing PEO thin films that have different ε values. With this method, LJ parameter at the simulated temperature 373 K are: σ_{PEO} = 3.76 Å and ε/k_B =154 K. These parameters yield a cohesive structure with a bulk density that most closely matches the experimental density of 1.06 g/cm^3.

Moves. Single bead and pivot move were used in order to improve the simulation efficiency. In a pivot move, bond vectors for a subchain of the original conformation were reversed to create a new configuration. A subchain with two to six beads was applied for pivot moves. For every Monte Carlo step (MCS), single bead moves and also multiple bead pivot moves were performed randomly. Every bead was tried once, on average, in both single bead moves and pivot moves. Therefore, a move of every bead was attempted twice, on average, within one MCS. Moves that cause double occupancy and collapses, which were caused by the overlap of backbone atoms after the reverse-mapping of the coarse-grained chains to the fully atomistic description, have been prohibited. The Metropolis criteria were applied to determine whether the move is made or not.

System Description. The simulations were performed in a periodic box with 20 unit lengths on each side of the lattice; i.e., $L_x x L_y x L_z = 20x20x20$. For all systems, a total of 1680 beads are put into this box to achieve the experimental density for PEO at 373 K. The size of 10 polymer chains are $N = 168$; i.e., all the molecules have 168 beads on the lattice. These beads can be reverse-mapped into 336 backbone atoms, $CH_3(OCH_2CH_2)_{111}OCH_3$. The initial configuration were randomly distributed in the periodic box. Next, a sufficiently long simulation was run until the system achieves equilibrium. After equilibration, an additional 10 million Monte Carlo Steps (MCS) are performed. The configurations are recorded every 10,000 MCS.

Energy Minimization of Reverse-Mapped Snapshots. Energy minimization (EM) of reverse-mapped snapshots is performed. The coordinates of the carbon/oxygen/hydrogen atoms in the chains that have been reverse mapped back onto the tetrahedral lattice were created by an in-house program. Then, energy minimization of the bulk snapshot was performed with the CVFF force field until the gradient is less than 0.1 kcal/(mol Å). In all steps, the steepest descents method is used if the gradient is greater than 1000 kcal/(mol Å), and conjugate gradient is used otherwise.

Results and Discussion

Equilibration of the System. Equilibration of the systems can be determined by evaluating the orientation autocorrelation functions (OACFS) defined using the end-to-end vector of the linear chain. The time constant for equilibration is the time required for the OACF to fall to $1/e$, and complete deconvolution of the end-to-end vectors from their initial orientations is obtained when the OACF reaches 0. The relaxation time for end-to-end vector was about $4.0x10^6$ MCS. In addition, the mean-square displacement of the center-of-mass ($g_{cm}(t)$) is evaluated to establish equilibrium conditions. When $g_{cm}(t)$ reaches the mean-square radius of gyration ($\langle R_g^2 \rangle$), the molecules have translated away from their initial positions. It was found that equilibration of the system by $4.9x10^6$ MCS is confirmed. The OACF and $g_{cm}(t)$ indicate that the movement of the chains equilibrates rapidly so 10^7 MCS were used for equilibration and other system properties were analyzed with an additional 10^7 MCS.

Chain Dimensions. A measure of the conformation of the individual chain in the bulk are its dimensions. The initial guess structures from Monte Carlo simulation gave the characteristic ratio, $C_n = \langle r^2 \rangle / nl^2$ and the radius of gyration, Rg, for chain with $X = 168$ as $C_n = 3.7 \pm 1.1$ ($\langle r^2 \rangle = 2661 \pm 1927$ Å^2) and $\langle Rg^2 \rangle^{1/2} = 20.7$ Å. These values are comparatively closed to ones calculated from RIS model of chains with similar geometry.

During the energy minimization, after the reverse-mapping, the overall shape of the chains did not change much. The dimensions are practically the same for the minimized structures as for the initial guesses e.g. $\langle Rg^2 \rangle^{1/2} = 26.8 \pm 6.0$ Å.

Distribution of Torsion Angles. After reverse mapping, but before EM, the distribution of torsion angles is limited to the three values that are allowed on the tetrahedral lattice. During the EM, the torsion system moves off-lattice. For the backbone atoms of PEO chains, there are two different types of dihedral angles defined by OC-CO and CO-CC atom sequences. In order to examine the conformations of PEO chains, the ensemble averaged population density distribution of these dihedral angles (ϕ) were calculated. Fig. 1 compares the population density distribution of dihedral angles along the OC-CO and CO-CC sequence in PEO. By our definition, the conformations are labeled *trans* (T) if $120° < \theta < 240°$, gauche plus (G^+) if $0° < \theta < 120°$, and gauche minus (G^-) if $240° < \theta < 360°$. The populations at G^+/G^- are nearly identical, as expected from the symmetry of the torsion potential energy function. The *trans* conformation of CO-CC bond is predominant, while *gauche* conformations (G^+ and G^-) give much smaller peaks near 80° and 280°, respectively. Neither G^+ nor G^- is favored. For the dihedral angles along the OC-CO atom sequence, the G^+ and G^- conformations are much more favored than T. This distribution is attributed to 'the gauche effect'. It is well accepted that when atoms at the two ends of a dihedral angle are very electronegative, the dihedral angle favors a *gauche* (G^+ or G^-) over the *trans* conformation despite the Coulombic repulsion between the two atoms. The direction and size of the most probable torsion angle for a G^+/G^- state are in excellent agreement with the expectation from the RIS model for PEO

Cohesive Energy Density and Solubility Parameters. The cohesive energy, U_{coh}, is the energy associated with the intermolecular interactions only and can be estimated by taking the difference between the total energy of the microstructure, U_{tot}, and that of the isolated parent chain, U_{par}. In order to determine the parent chain energy, the cube edge length was simply set to a very large value so that the chain was fully enclosed in the box and did not interact with its image. Hildebrand's solubility parameter, δ, is the square root of the cohesive energy density, and $\delta = \left(\frac{U_{par} - U_{tot}}{V} \right)^{1/2}$ where V being the volume of the microstructure. The average Hildebrand solubility parameter is $\delta = 10.02$ cal$^{1/2}$/cm$^{3/2}$ (van der Waals = 9.46, electrostatic = 3.32 cal$^{1/2}$/cm$^{3/2}$). The reported experimental values for the solubility parameters of PEO are about 9.8 cal$^{1/2}$/cm$^{3/2}$, in agreement with the estimated results.

Atomic Pair Distribution Functions. The pair correlation function gives a measure of the probability that, given the presence of an atom at the origin of an arbitrary reference frame, there will be an atom with its center located in a spherical shell of infinitesimal thickness at a distance r from the reference atom. This concept also embraces the idea that the atom at the origin and the atom at distance r may be of different chemical types, say α and β. The resulting function is then commonly given the symbol $g_{\alpha\beta}(r)$. It is also sometimes referred to as the radial distribution function (RDF). RDF calculations provide insights into the PEO structures by reporting the relative density of atom pairs separated by a distance r according to: $g(r) = \frac{V}{N} \left\langle \sum_i \sum_{j \neq i} \delta(r - r_{ij}) \right\rangle$ where i and j refer to the ith and jth molecules and the angle

brackets imply averaging over different configurations. These functions give a way to infer interactions between atoms. RDF for three different pairs of elements (CC, CO and OO) are shown in Figure 2. The curves are obtained by averaging the results of energy-minimized snapshots (20 snapshots at 0.75 g/cm^3). They include only pairs that depend on the conformation of the polymer chain. The portion of the pair distribution function that is not dependent on conformation would appear as "Dirac spikes" in the figure. The first peak in these pair distribution functions occurs between 4 and 5 Å and is indicative of nearest-neighbor chain packing. The distance is less than that seen for the first peak in the C-C pair distribution function in normal alkane where the peak occurs at distances greater than 5 Å. The closer chain packing in PEO reflects the greater density of the PEO systems. The height of the first peak in the C-C distribution is greater in PEO melts than was observed in polymethylene melts.

Neutron Structure Factor. From the elemental pair distribution functions, it is straightforward to extract scattering patterns. The direct comparison of theoretical against experimental diffraction results constitutes a useful check for the structural predictions of the model. Technically, the scattering curve, $I(Q)$, for a material is related by a Fourier transform operation to the radial distribution function. For an isotropic amorphous structure, the curve may be expressed in the explicit form: $I(Q) = \sum_j \sum_k \frac{f_j f_k \sin(Qr_{jk})}{Qr_{jk}}$

where Q is the magnitude of the scattering vector (= $4\pi\sin\theta/\lambda$) with 2θ the scattering angle and λ the radiation wavelength, and where the indices j and k extend over all atoms in all molecules. The scattering amplitudes have been taken as: f_H = -3.74, f_O = 5.80 and f_C = 6.65 fermi. The calculated spectrum is shown in Figure 3. It exhibits five peaks at Q = 0.58, 1.53, 3.07, 5.32 and at 8.79 Å^{-1}. These locations fit the experimentally observed peaks that occur at Q = 0.6, 1.33 and at 3.0 Å^{-1} very well. The major difference between prediction and experiment lies in the intensity of the signal at lowest Q that is much stronger in the calculated spectrum. However, the distances most relevant for diffraction at Q = 0.8 Å^{-1} are close to half of the cube edge and aberrations are to be expected. The agreement between the experimental $I(Q)$ function and that from the MC/MM simulations is reasonable agreement, further validating the generation method of amorphous PEO structure.

Acknowledgement: This work is supported by NSRC (Grant number 2-2548/PS02)

Conclusion. This work illustrate a multiscale molecular modeling technique for polymer simulation. A large amorphous PEO structure was generated using a combination of MC/MM technique. The equilibrated structure from MC was reverse-mapped to a fully atomistic structure. The subsequent EM produces a reasonable minor adjustment in the coordinates when it converts the system to an off-lattice representation.

References

1. J. Baschnagel, K. Binder, P. Doruker, A.A. Gusev, O. Hahn and K. Kremer *et al.*, Bridging the gap between atomistic and coarse-grained models of polymers, Adv Polym Sci 152, 41, (2000).
2. V. Vao-soongnern, P. Doruker, W. L. Mattice, *Computational Studies, Nanotechnology, and Solution Thermodynamics of Polymer Systems*, Kluwer Academic/Plenum Publishers, New York, 117, (2001).

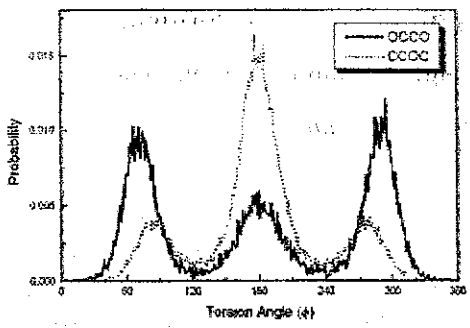

Fig. 1. Average population density distribution of dihedral angles along the CO-OC and CO-CC backbone atom sequence for PEO after MC/MM equilibration and minimization.

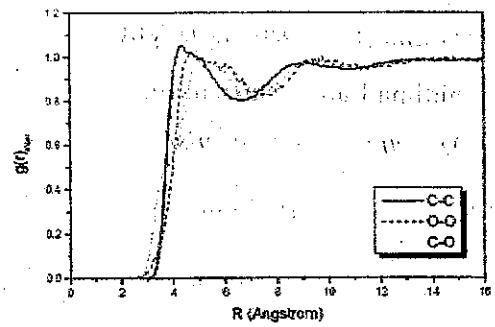

Figure 2 Intermolecular C-C, O-O and C-O pair distribution for amorphous PEO melts as a function of separation distance after MC/MM equilibration and minimization.

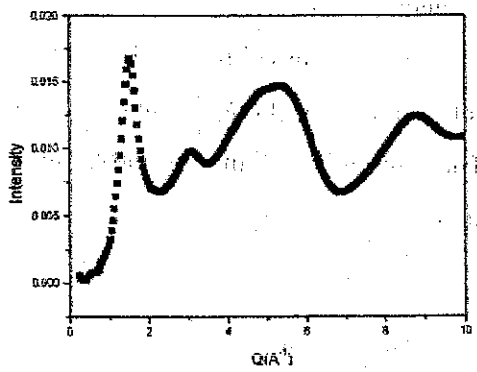

Figure 3 Static normalized coherent structure factor $I(Q)$ for neutron diffraction calculated after MC/MM equilibration and minimization.